Effect of frequency detunings and finite relaxation rates on laser localized structures

S. V. Fedorov,[1,*] A. G. Vladimirov,[2,†] G. V. Khodova,[1] and N. N. Rosanov[1,‡]
[1]*Institute for Laser Physics, Vavilov State Optical Institute, Birzhevaya line 12, 199034 St. Petersburg, Russia*
[2]*Physics Faculty, St. Petersburg State University, 1 Ulianovskaya Street, 198904 St. Petersburg, Russia*
(Received 17 June 1999)

We study, analytically and numerically, the effect of frequency detunings and relaxation processes in laser media on stability and bifurcations of dissipative optical localized structures (DOLS's) in a transversely one-dimensional laser with a saturable absorber. The approximate envelope equation, with an intensity dependent effective coefficient of the diffusion, is derived. Andronov-Hopf bifurcations resulting from frequency detuning and leading to oscillatory DOLS's are analyzed numerically. A numerical and analytical study of bifurcations of transversely motionless DOLS's in a laser with finite relaxation rates of amplifying and absorbing media is performed. New types of DOLS's are found, including those moving with a large transverse velocity and those moving with a periodically oscillating transverse velocity. Hysteresis between different types of DOLS's is demonstrated.

PACS number(s): 42.65.Tg, 42.65.Sf, 42.65.Pc, 42.55.Ah

I. INTRODUCTION

Dissipative localized (solitonlike) structures of laser radiation are of particular interest because they represent self-organization in dissipative nonlinear systems with energy exchange [1,2], and are promising for applications in optical data processing [3]. The term ''dissipative,'' in contrast to ''conservative,'' underlines a key part of the energy flows in systems with radiation sinks (losses) and sources (external radiation injection or pumping). While conservative solitons in transparent nonlinear media (e.g., solitons of the nonlinear Schrödinger equation [4]) have a continuous spectrum of their parameters, including the peak intensity, a spectrum of the main characteristics of the dissipative optical localized structures (DOLS's or ''autosolitons'') is discrete, since the condition of balance between losses and pumping is fulfilled only for some definite values of the radiation intensity. Therefore, the physics of the DOLS's differs essentially from that of the conservative solitons. As for applications, the effect of noise and the drift of parameters are significantly reduced for the DOLS's, resulting in their robustness and extreme stability.

In optics, stationary and pulsating dissipative localized structures were first predicted theoretically [5,6] and found experimentally [7,8] for passive nonlinear systems, such as wide-aperture nonlinear interferometers driven by external radiation (see also Ref. [9] and Ref. [3], and references therein). Due to the important role of diffraction in their formation, these structures were called ''diffractive autosolitons.'' Diffusive autosolitons were investigated earlier in various physical, chemical, and biological systems [10,11]. Mathematical aspects of theory of similar structures were also studied without any reference to optical problems (see Refs. [12,13], and references therein). Specific features of DOLS's in conditions of ''nascent'' bistability were considered in Ref. [14]. Different applications of the DOLS's to information processing were proposed, including a shift register and full adder (see Refs. [9] and [15]. In experiment, a scheme of multichannel optical memory was demonstrated in Refs. [7,8].

Similar types of DOLS's—the so-called ''laser autosolitons''—were first predicted in Ref. [16]. In this paper localized structures of laser radiation were theoretically found in a model of a wide-aperture laser with a saturable absorber under bistability conditions. Recently such structures, with a hard type of excitation, were observed experimentally in a cavity with photorefractive crystals that served as gain and loss elements [17,18], and in a dye laser with bacteriorhodopsin as a saturable absorber [19]. In subsequent studies different types of laser DOLS's were found and investigated: geometrically one-dimensional (1D), (2D), and (3D), stationary and pulsating, motionless and moving, radially symmetric and rotating, with high-order topological indices, and solitary and coupled [20,21,9,3,22].

In the case of fast nonlinearity the governing equations for cavity systems with diffraction and for continuous media with frequency dispersion are equivalent. Therefore, temporal DOLS's in a single-mode nonlinear fiber with saturable gain and losses are mathematically equivalent to 1D spatial cavity DOLS's in a laser with a saturable absorber (see Ref. [9] and Ref. [3], and references therein). In Ref. [23] a specific case of a fiber with large frequency detunings, dominating a dispersive type of inertionless optical nonlinearity, was considered. For practical purposes, detunings between the radiation carrier frequency and the frequencies of amplification and absorption spectral line centers cannot be too large. Otherwise the radiation amplification would not be efficient.

An essential limitation of the existing theory of laser DOLS's is the lack of a systematic study of the effect of frequency detunings and relaxation times of the active and passive media on the DOLS properties. Most previous studies were performed under the assumption that relaxation processes in the laser media can be neglected. However, our recent numerical study [24] showed that even the very small relaxation times of the media drastically change the proper-

*Electronic address: sfedorov@sf3997.spb.edu
†Electronic address: andrei@sp1254.spb.edu
‡Electronic address: rosanov@ilph.spb.su

ties of the DOLS's, including their symmetry features, stability, spectrum of characteristics, etc. In experiments [17–19], a saturable absorber is characterized by very large relaxation times (in the range of seconds), much greater than the cavity relaxation time. In Ref. [25] a different type of DOLS's corresponding to an opposite case of a very long relaxation time of an active medium, was studied in a laser without a saturable absorber. However, these structures are unstable because of the growth of initially small perturbations at the structure periphery [3].

The goal of this paper is to study the stability and bifurcations of localized structures (''laser DOLS's'') in a wide-aperture laser with a saturable absorber, taking into account the effect of frequency detunings and population relaxation processes (a class B laser). We consider the simplest case of 1D DOLS's corresponding to a single mode regime for one of the two transverse coordinates. The bifurcation approach used here is similar to that developed earlier for class A lasers in Ref. [26].

Starting with Maxwell-Bloch equations and assuming small relaxation times, in Sec. II we derive approximate envelope equations for a wide-aperture laser with a saturable absorber. The simplest (plane-wave monochromatic) solutions of these equations are analyzed in Sec. III. In Sec. IV we consider laser DOLS's for the case of media inertionless nonlinearity; the effect of frequency detunings on the DOLS bifurcations is investigated. Section V is devoted to the effect of population relaxation rates on the DOLS stability and bifurcations. The stability domains of different types of DOLS's are given, and various hysteretic phenomena resulting from overlapping of these domains are described. Conclusions are given in Sec. VI.

II. LASER MODEL

We consider a wide-aperture laser with an intracavitary saturable absorber. In the mean-field approximation [27] valid for the case of small changes of the radiation field per one cavity roundtrip, the Maxwell-Bloch equations have the forms

$$\frac{\partial E}{\partial t} - i\frac{\partial^2 E}{\partial x^2} = P_g - P_a - E, \tag{2.1a}$$

$$\tau_g \frac{\partial g}{\partial t} = g_0 - g - \mathrm{Re}(EP_g^*), \tag{2.1b}$$

$$\tau_a \frac{\partial a}{\partial t} = a_0 - a - b\ \mathrm{Re}(EP_a^*), \tag{2.1c}$$

$$\tau_{\perp g}\frac{\partial P_g}{\partial t} = gE - (1+i\Delta_g)P_g, \tag{2.1d}$$

$$\tau_{\perp a}\frac{\partial P_a}{\partial t} = aE - (1+i\Delta_a)P_a. \tag{2.1e}$$

Here E is the dimensionless complex electric field envelope; g (a) is the population difference in an active (passive) medium; and g_0 and a_0 are stationary values of the population differences in the absence of the laser field ($E=0$), which are proportional to small signal coefficients of gain and absorption, respectively. The time t is normalized by the cavity relaxation time, and x is the dimensionless transverse coordinate normalized by the width of the effective Fresnel zone

$$X_F = \sqrt{\frac{L_c}{2k_0(1-R)}},$$

where L_c is the cavity length, k_0 is the light wave number, and R is the product of the cavity mirror coefficients of reflection. The ratio parameter $b=\tau_a\tau_{\perp a}\mu_a^2/(\tau_g\tau_{\perp g}\mu_g^2)$ measures the relative saturability of active and passive media. Here $\mu_{g,a}$ are the atomic dipole momenta, and $\tau_{\perp g,\perp a}, \tau_{g,a}$ are the relaxation times for atomic polarizations and population differences divided by the cavity relaxation time. $P_{g,a}$ are the envelopes of atomic polarizations, and $\Delta_g=(\omega_g-\omega_c)\tau_{\perp g}$ and $\Delta_a=(\omega_a-\omega_c)\tau_{\perp a}$ are dimensionless detunings between the gain (absorption) spectral line center $\omega_{g,a}$ and the frequency of empty cavity mode ω_c. Model (2.1) corresponds to the case of homogeneous spectral broadening; particle diffusion is neglected here. We consider a wide-aperture laser with a planar cavity width much greater than X_F.

Let us consider a class B laser for which the media polarization relaxation times are much smaller than the cavity relaxation time, while the population relaxation times $\tau_{g,a}$ are in general large enough: $\tau_{\perp g,\perp a}\ll 1$. Using the approach developed in Ref. [28], we take into account the effects of polarization relaxation in the first-order approximation in $\tau_{\perp g,\perp a}$ only. In zeroth order, polarization is determined by equating the left hand side of Eq. (2.1d) to zero: $P_g^{(0)}=(1+i\Delta_g)^{-1}gE$. Up to the first-order terms in $\tau_{\perp g}$, from Eq. (2.1d) we obtain

$$P_g^{(1)} = P_g^{(0)} + \tau_{\perp g}(1+i\Delta_g)^{-1}\left(\frac{\partial P_g^{(0)}}{\partial t}\right). \tag{2.2}$$

Similar relations are valid for a passive medium. Substituting Eq. (2.2) into Eq. (2.1a), we keep only the first-order terms in $\tau_{\perp g,\perp a}$ before the second derivative on x. Moreover, we neglect the imaginary parts of these terms acting as small perturbations to the diffraction coefficient. These assumptions are justified, because it is precisely the real part of these terms that gives an effective coefficient of diffusion, which has a critical effect on the stability of spatially homogeneous regimes [28]. Finally we obtain the following system of equations governing the evolution of the transverse field distribution in a class B laser with a saturable absorber:

$$\frac{\partial \overline{E}}{\partial t} - (i+d)\frac{\partial^2 \overline{E}}{\partial x^2} = [-1+(1-i\Delta_g)\overline{g}-(1-i\Delta_a)\overline{a}]\overline{E}, \tag{2.3a}$$

$$\tau_g\frac{\partial \overline{g}}{\partial t} = \overline{g}_0 - (1+I)\overline{g}, \tag{2.3b}$$

$$\tau_a\frac{\partial \overline{a}}{\partial t} = \overline{a}_0 - (1+\overline{b}I)\overline{a}, \tag{2.3c}$$

$$d=2[\tau_{\perp a}\overline{a}\Delta_a/(1+\Delta_a^2)-\tau_{\perp g}\overline{g}\Delta_g/(1+\Delta_g^2)], \quad (2.4)$$

where $I=|\overline{E}|^2$ is the laser field intensity for a normalized amplitude $\overline{E}=E/\sqrt{1+\Delta_g^2}$; and $\overline{g}=g/(1+\Delta_g^2)$ and $\overline{a}=a/(1+\Delta_a^2)$ are the saturated gain and absorption coefficients at the cavity frequency. Since one has to use saturated values of populations in Eq. (2.4), the diffusion coefficient $d=d(I)$ in Eq. (2.3a) is intensity dependent. The normalized linear gain and absorption coefficients, $\overline{g_0}$ and $\overline{a_0}$, and the ratio of the saturation intensities $\overline{b}$ at the cavity frequency are defined by

$$\overline{g_0}=g_0/(1+\Delta_g^2), \quad \overline{a_0}=a_0/(1+\Delta_a^2),$$
$$\overline{b}=b(1+\Delta_g^2)/(1+\Delta_a^2). \quad (2.5)$$

In the limit of inertionless media ($\tau_{g,a}\to 0$) we find, from Eqs. (2.3b) and (2.3c),

$$\overline{g}(I)=\overline{g_0}/(1+I), \quad \overline{a}(I)=\overline{a_0}/(1+\overline{b}I). \quad (2.6)$$

Then Eqs. (2.3a) and (2.4) are reduced to a single equation for the electric field envelope:

$$\frac{\partial\overline{E}}{\partial t}-[i+d(|\overline{E}|^2)]\frac{\partial^2\overline{E}}{\partial x^2}=f(|\overline{E}|^2)\overline{E}, \quad (2.7)$$

where

$$f(I)=-1+\frac{(1-i\Delta_g)\overline{g_0}}{1+I}-\frac{(1-i\Delta_a)\overline{a_0}}{1+\overline{b}I}, \quad (2.8a)$$

$$d(I)=-2\left(\frac{\tau_{\perp g}\Delta_g\overline{g_0}}{(1+\Delta_g^2)(1+I)}-\frac{\tau_{\perp a}\Delta_a\overline{a_0}}{(1+\Delta_a^2)(1+\overline{b}I)}\right). \quad (2.8b)$$

Note that unlike the amplitude equations of Ginzburg-Landau type, where $f(I)$ and $d(I)$ are expanded in power series, Eq. (2.7) is valid not only in a small vicinity of the bistability threshold. Therefore, Eq. (2.7) describes a wider domain of DOLS stability, and is more adequate to the experimental situation. The next simplification is to neglect the intensity dependence of the diffusion coefficient d in Eq. (2.7). A justification of this assumption will be given in Sec. V C. Note that when the diffusion coefficient defined by Eq. (2.8b) is not positive, additional terms with fourth-order derivatives must be included in Eq. (2.2) [28].

In the simplest case, when the small diffusion coefficient is neglected ($d=0$), instead of Eq. (2.7) we have

$$\frac{\partial\overline{E}}{\partial t}-i\frac{\partial^2\overline{E}}{\partial x^2}=f(|\overline{E}|^2)\overline{E}. \quad (2.9)$$

Equations (2.3a), (2.4), and (2.9) are invariant under a phase shift of the field envelope, translations, and reflections in space. These symmetries are defined by the transformations

$$\overline{E}(x,t)\to\overline{E}(x,t)e^{i\eta}, \quad (2.10a)$$

$$x\to x+h, \quad (2.10b)$$

$$x\to -x, \quad (2.10c)$$

with arbitrary η and h.

Moreover, Eq. (2.9) describing a laser with inertionless media exhibits additional symmetry with respect to ''Galilean transformation'' to a reference frame moving in the transverse direction with velocity v:

$$\overline{E}(x,t)\to\overline{E}(x-vt,t)e^{ivx/2-iv^2t/4}. \quad (2.11)$$

This means that any motionless solution of Eq. (2.9) generates a family of uniformly moving field distributions, each characterized by some value of the velocity v (a continuous spectrum of v). For nonzero values of the relaxation times $\tau_{g,a}$, symmetry (2.11) is broken and, hence, DOLS's cannot travel with an arbitrary constant velocity. In this case uniformly moving DOLS's are expected to have zero velocity or some fixed nonzero velocity.

III. MONOCHROMATIC PLANE-WAVE SOLUTIONS

Stationary spatially homogeneous solutions of Eqs. (2.1) are obtained by equating their right hand sides to zero. After the substitutions

$$E(x,t)\to e^{-i\theta t}\sqrt{\tilde{I}},$$
$$P_g(x,t)\to e^{-i\theta t}\sqrt{\tilde{I}}g(\tilde{I})/(1+i\Delta_g-i\theta\tau_{\perp g}),$$

where $\tilde{I}=I(1+\Delta_g^2)$ is proportional to a plane wave intensity and θ is the wave frequency shift with respect to the cavity eigenfrequency, we obtain

$$-1+i\theta+\frac{(1-i\Delta_g+i\theta\tau_{\perp g})g_0}{1+(\Delta_g-\theta\tau_{\perp g})^2+\tilde{I}}-\frac{(1-i\Delta_a+i\theta\tau_{\perp a})a_0}{1+(\Delta_a-\theta\tau_{\perp a})^2+b\tilde{I}}=0. \quad (3.1)$$

For class B lasers ($\tau_{\perp g}\to 0$, $\tau_{\perp a}\to 0$), the complex equation (3.1) is separated into two real equations for the wave intensity I and the frequency shift θ:

$$\mathrm{Re}\, f(I)=0, \quad \theta=-\mathrm{Im}\, f(I), \quad (3.2)$$

where $f(I)$ is defined in Eq. (2.8a). In doing so we neglect off-resonant solutions [29] and take into account the resonant ones only. Generally for the latter solutions the frequency shift θ differs from zero only for nonzero values of frequency detunings $\Delta_{g,a}$. Using the rescaled media parameters (2.5) evaluated at the cavity eigenfrequency, it is possible to solve equations (3.2) for arbitrary values of detunings $\Delta_{g,a}$ in the same way as for zero detunings. Two solutions of the corresponding quadratic equation for I, if they exist and are positive, determine the upper and intermediate intensity branches (see Fig. 1). Their stability will be discussed later. The lower branch corresponds to the nonlasing regime, $I=0$. Hysteresis takes place in the range $g_{\mathrm{down}}<\overline{g_0}<g_{\mathrm{up}}$. Here $g_{\mathrm{up}}=1+\overline{a_0}$ is the linear lasing threshold, and $g_{\mathrm{down}}=(1+\sqrt{\overline{a_0}a_{\mathrm{thr}}})^2/(\overline{b}a_{\mathrm{thr}})$ is the threshold of lasing breakdown. The intensity corresponding to the lasing breakdown

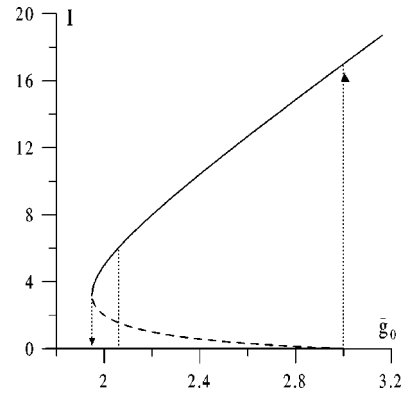

FIG. 1. Intensity of the plane-wave regime vs linear gain coefficient $\bar{g}_0$. The lower hysteretic branch $I=0$ is stable up to the right vertical dashed straight line. The regimes represented by the upper hysteretic branch exist and are stable against small spatially uniform perturbations up to the left vertical dashed straight line. The dashed curve corresponds to the intermediate unstable branch. The vertical straight line lying inside the bistability range corresponds to $\bar{g}_0=2.06$. Parameters are: $\bar{a}_0=2$ and $\bar{b}=10$.

is $I_{\mathrm{down}}=(\sqrt{\bar{a}_0/a_{\mathrm{thr}}}-1)/\bar{b}$, where $a_{\mathrm{thr}}=1/(\bar{b}-1)$ is the threshold value of the absorption coefficient. Bistability exists if the two conditions are satisfied: (i) saturation intensity for a passive medium is less than that for an active medium, $\bar{b}>1$; and (ii) the linear absorption coefficient is large enough, $\bar{a}_0>a_{\mathrm{thr}}$.

In Fig. 2 the boundaries of bistability domain are shown in the $\{\Delta_g, \Delta_a\}$ plane. They are determined by the equation $g_{\mathrm{up,down}}(\Delta_g^2,\Delta_a^2)=g_0/(1+\Delta_g^2)$, which can be resolved with respect to Δ_g^2. As a result, the condition of the lasing breakdown is represented by a straight line in the plane of detunings squared:

$$\Delta_g^2=-1+g_0+(1+\Delta_a^2+a_0)/b-2\sqrt{g_0a_0/b}. \quad (3.3)$$

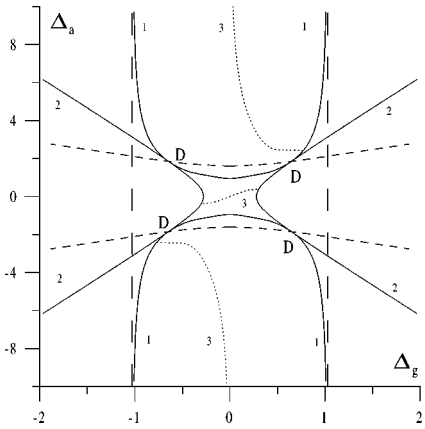

FIG. 2. Bistability and modulation instability domains in the plane of detunings. Curves 1 indicate the linear lasing threshold. Curves 2 correspond to the threshold of lasing breakdown. Vertical dashed straight lines are asymptotes of curves 1. Symbols *D* denote tangent points of these curves. Bistability domains are situated near zeroth detunings. The modulation instability domain lies to the right of dotted curve 3. Parameter values are chosen in such a way that bistability exists for zero detunings: $g_0=2.06$, $a_0=2$, and $b=10$.

In the $\{\Delta_g, \Delta_a\}$ plane this boundary is given by curve 2. The equation for the lasing threshold determines a hyperbola, or curve 1 in Fig. 2:

$$\Delta_g^2=-1+\frac{(1+\Delta_a^2)g_0}{1+\Delta_a^2+a_0}. \quad (3.4)$$

Equations (3.3) and (3.4) are tangent to one another at the symmetrical points $D(\Delta_g,\Delta_a)$:

$$\Delta_g^2=-1+g_0-\sqrt{g_0a_0/b}, \quad \Delta_a^2=-1-a_0+\sqrt{g_0a_0/b}.$$

In the domain of small detunings, bounded by curves 1 and 2, the absorptive mechanism of nonlinearity has a dominant role. The transition from small to large detunings corresponds to a transition from absorptive to dispersive types of nonlinearity. However, bistability is absent in areas of large detunings, between curves 1 and 2, because the necessary condition of bistability, $I_{\mathrm{down}}>0$, or $\bar{a}_0=a_0/(1+\Delta_a^2)>a_{\mathrm{thr}}$, is not fulfilled there. As follows from Fig. 2, the last condition also depends on the detunings. The dashed lines (parabolic curves in the plane of squared detunings), correspond to the condition $\bar{a}_0=a_{\mathrm{thr}}$, and intersect the boundaries of the bistability domain in tangent points *D*. They enclose the bistability domain in the case of large detunings Δ_a. Nevertheless, bistability can also be obtained in the region of large detunings, since with an increase of the gain coefficient g_0 tangent points go to the region of large detunings along the unchanged dashed lines. In this case the bistability domain does not include the vicinity of zero detunings, and breaks into two parts, corresponding to opposite signs of Δ_g.

Now let us consider stability of the plane-wave solutions against small perturbations (modulation instability). Linearizing Eq. (2.9) with respect to perturbations of the type

$$\bar{E}(x,t)\to e^{i\theta t}\sqrt{I}(1+u_1e^{\gamma t+i\kappa x}+u_2^*e^{\gamma^* t-i\kappa x}),$$

one can find an expression for the dependence of perturbation growth rate γ on modulation spatial frequency κ:

$$\gamma(\kappa^2)=\mathrm{Re}[If'(I)]+\sqrt{\mathrm{Re}[If'(I))^2+2\kappa^2\,\mathrm{Im}[If'(I)]-\kappa^4}. \quad (3.5)$$

It follows from Eq. (3.5) that modulation instability exists in the range $0<\kappa^2<2\kappa_{\max}^2$, when $\mathrm{Im}[If'(I)]>0$. Here $\kappa_{\max}^2=\mathrm{Im}[If'(I)]$. The maximum growth rate is given by $\gamma(\kappa_{\max}^2)=\mathrm{Re}[If'(I)]+\sqrt{\mathrm{Re}[If'(I)]^2+\kappa_{\max}^2}>0$. Curve 3 in Fig. 2 is determined by the condition $\mathrm{Im}[f'(I)]=0$. Since positive values Δ_g correspond to radiation self-focusing in the active medium, the domain of modulation instability appears to the right from dotted curve 3.

IV. LOCALIZED STRUCTURES FOR INERTIONLESS NONLINEARITY: EFFECT OF FREQUENCY DETUNINGS

The simplest type of stationary localized structure is a motionless DOLS. The steady-state envelope of such a DOLS does not depend on the values of the relaxation times $\tau_{g,a}$, whereas its stability is relaxation dependent. In this section we consider the stability and bifurcations of a stationary DOLS for the case of inertionless nonlinearity. For zero

frequency detunings such a study was performed in Refs. [26,30]. Therefore, here we concentrate on the case of nonzero frequency detunings. In dimensional units, the width of the DOLS is typically about the effective Fresnel zone X_F, and depends slightly on gain. Note that laser DOLS's exist both without and with a modulational instability of homogeneous field distributions, as well as in the case of driven nonlinear interferometers [31,32].

For $d=0$ we seek for solution of Eq. (2.7) in the form

$$\overline{E}=A(x)e^{-i\alpha t}, \tag{4.1}$$

with $A(x)\to 0$ for $x\to\pm\infty$. Substituting Eq. (4.1) into Eq. (2.9), we obtain the following ordinary differential equation for the DOLS envelope:

$$\frac{d^2A}{dx^2}+\alpha A-iAf(|A|^2)=0, \tag{4.2}$$

with $f(|A|^2)$ defined by Eq. (2.8a). The value of the spectral parameter α describing the frequency shift of the DOLS is to be determined. After the substitution $A(x)=\rho(x)e^{i\Phi(x)}$, Eq. (4.2) can be rewritten in the forms [13,26]

$$\begin{aligned}\partial_x\rho&=\rho k,\quad \partial_x q=-2qk+\mathrm{Re}\, f(\rho^2),\\ \partial_x k&=-\alpha+q^2-k^2-\mathrm{Im}\, f(\rho^2),\end{aligned} \tag{4.3}$$

where $q=\partial_x\Phi$, $k=\rho^{-1}\partial_x\rho$, and $\partial_x\equiv\partial/\partial x$.

Equations (4.3) have two spatially homogeneous solutions $L_\pm$ which correspond to zero laser field: $\rho=0$, $q_\pm=\pm(\frac{1}{2}[(\alpha+f_{02})^2+{f_{01}}^2]^{1/2}+\alpha+f_{02})^{1/2}$, and $k_\pm=f_{01}/2q_\pm$. Here $f_{01}=\mathrm{Re}\, f(0)=-1+\overline{g}_0-\overline{a}_0$ and $f_{02}=\mathrm{Im}\, f(0)=-(\overline{g}_0\Delta_g-\overline{a}_0\Delta_a)$. These two solutions represent the nonlasing regime; see Sec. III. Linearization of Eqs. (4.3) in the vicinities of the fixed points $L_\pm$ shows that each of the solutions $L_\pm$ has a single real eigenvalue and a pair of complex conjugated eigenvalues defined by $\lambda_1^\pm=k_\pm$, $\lambda_2^\pm=-2(k_\pm+iq_\pm)$, and $\lambda_3^\pm=\lambda_2^{\pm *}$. Since in the bistability domain we have $f_{01}<0$, the fixed point L_- (L_+) is a saddle-focus with a 1D unstable (stable) manifold and a 2D stable (unstable) manifold.

A stationary DOLS corresponds to heteroclinic trajectory of Eqs. (4.3) connecting the fixed points L_+ and L_-. Therefore, we need to find bifurcation points in the parameter space for which Eqs. (4.3) have a heteroclinic trajectory of the type described. Specifically, a fundamental (single-humped) DOLS corresponds to the simplest (''single-pass'') heteroclinic trajectory that visits vicinities of the fixed points L_- to L_+ only once. It was shown in Ref. [26] that the existence of such a DOLS implies the existence of an infinite number of multi-humped, or combined DOLS's, that can be considered as a coupled state of two or more single DOLS's. Due to the symmetry property (2.11), after an appropriate shift along the x axis the envelope $A(x)$ of the motionless DOLS can be taken as either even or odd function of x. Note that, according to Ref. [26], the intensity of any stationary DOLS cannot have more than one zero at a finite transverse coordinate x. Hence for an odd function $A(x)$ there is only one zero at $x=0$, and no zeros for even functions $A(x)$. In particular, for the symmetric [with an even function $A(x)$] three-particle DOLS shown in Fig. 3, there are no exact intensity zeros. As follows from Fig. 3(b), the zeros of real and imaginary parts of the complex envelope $A(x)$ are slightly split. Note that Fig. 3 presents results of a direct solution of the partial differential equation (2.9). We solve this and similar equations (2.3) numerically by the splitting method, with the use of an algorithm of fast discrete Fourier transformation [6,16].

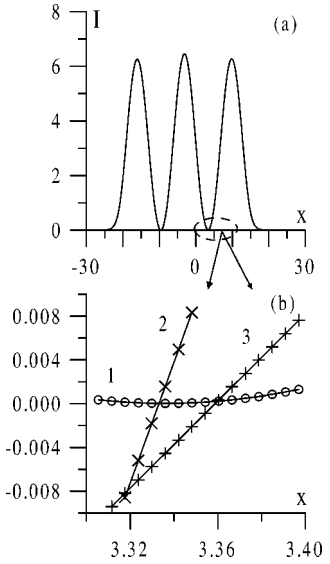

FIG. 3. Stable three-particle localized structure. Curve 1 represents transverse intensity profiles. Curve 2 (3) shows the real (imaginary) part of the field envelope near one of the two intensity minima. Markers represent calculation mesh. Parameters are the same as in Fig. 2.

Now let us consider the DOLS stability against small perturbations. In this section we deal with the simplest case of inertionless media, when the laser dynamics is described by Eq. (2.9). An unperturbed solution has the form of Eq. (4.1), with the envelope $A(x)$ obeying Eq. (4.2). Substituting slightly perturbed solutions

$$[\mathbf{V}_0(x)+\delta\mathbf{V}(\mathbf{x})e^{\lambda t}]e^{-i\alpha t},\quad \mathbf{V}_0=\begin{pmatrix}\mathrm{Re}\, A\\ \mathrm{Im}\, A\end{pmatrix},\quad \delta\mathbf{V}=\begin{pmatrix}\mathrm{Re}\ \delta A\\ \mathrm{Im}\ \delta A\end{pmatrix} \tag{4.4}$$

into real and imaginary parts of Eq. (2.9) and neglecting second and higher terms with respect to small perturbation $\delta\mathbf{V}$, we obtain the linear equation $\hat{L}_0\delta\mathbf{V}(x)=\lambda\,\delta\mathbf{V}(x)$ for the eigenvalues λ, determining the stability of the DOLS. Here the linear operator

$$\hat{L}_0=\begin{pmatrix}\mathrm{Re}\, F_+(A,A^*) & -\alpha-\partial_{xx}-\mathrm{Im}\, F_-(A,A^*)\\ \alpha+\partial_{xx}+\mathrm{Im}\, F_+(A,A^*) & \mathrm{Re}\, F_-(A,A^*)\end{pmatrix}, \tag{4.5}$$

with $F_\pm(A,A^*)=f(I_0)+f'(I_0)(I_0\pm A^2)$, $I_0=|A|^2$, and $f'(I_0)=(df(I)/dI)_{I=I_0}$.

In the bistability domain, where the nonlasing regime $A=0$ is stable, the continuous spectrum of operator (4.5) lies in the left half-plane of the complex plane $\lambda=\mathrm{Re}\,\lambda+i\,\mathrm{Im}\,\lambda$,

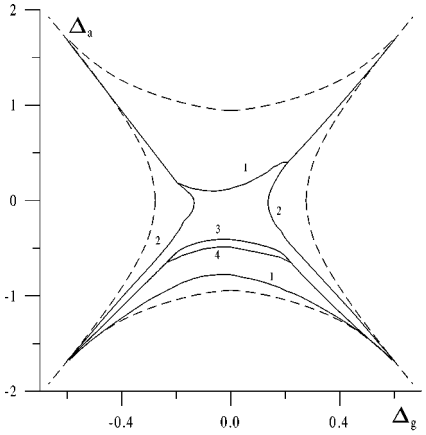

FIG. 4. Stability boundaries of the localized structures on the plane of frequency detunings. The localized structure is stable for moderate values of detunings. Dashed lines indicate the boundaries of the bistability domain of spatially homogeneous regimes. Curves 1 represent the Andronov-Hopf supercritical bifurcation. At saddle-node bifurcation curves 2, a stable localized solution merges with an unstable one and disappears. Curves 3 and 4 are the upper and lower boundaries of the stability domain of an oscillating localized structure. Below curve 4 an oscillating localized structure is transformed into a ''leading center.'' Bistability of stationary and oscillating localized structures takes place between curve 3 and the lower part of curve 1. A narrow bistability domain near upper curve 1 is not shown. Parameters are the same as in Fig. 2.

and does not produce instability. Therefore, we can restrict our consideration to the discrete spectrum.

Due to the symmetry properties (2.10) and (2.11), the discrete spectrum of operator (4.5) includes a triply degenerate zero eigenvalue. Two corresponding eigenvectors, or ''neutral modes,'' are designated by $\mathbf{\Psi}_{1,2}(x) = (\mathrm{Re}\,\psi_{1,2}, \mathrm{Im}\,\psi_{1,2})^T$, with $\psi_1 = iA$ and $\psi_2 = \partial_x A$. These eigenvectors obey the equation $\hat{L}_0 \mathbf{\Psi}_{1,2}(x) = 0$. The third zero eigenvalue is associated with the symmetry property (2.11), and corresponds to the adjoint vector $\mathbf{\Psi}_3(x) = (\mathrm{Re}\,\psi_3, \mathrm{Im}\,\psi_3)^T$ with $\psi_3 = -ixA/2$ obeying the equation $\hat{L}_0 \mathbf{\Psi}_3(x) = \mathbf{\Psi}_2(x)$. Note that, due to the symmetry property of the fundamental DOLS envelope $A(-x) = \pm A(x)$, the two neutral modes $\mathbf{\Psi}_1(x)$ and $\mathbf{\Psi}_2(x)$ have opposite parities. Specifically, for a ''one-particle'' DOLS with an even function $A(x) = A(-x)$, we have $\mathbf{\Psi}_1(x) = \mathbf{\Psi}_1(-x)$ and $\mathbf{\Psi}_2(x) = -\mathbf{\Psi}_2(-x)$. Moreover, since $\hat{L}_0(x) = \hat{L}_0(-x)$, any eigenvector of the linear operator $\hat{L}_0$ is either even or odd. Therefore, it is possible to study the stability with respect to even (symmetric) and odd (antisymmetric) perturbations separately.

The discrete spectrum of the linear operator (4.5) λ was calculated numerically for a fundamental DOLS with different frequency detunings Δ_g and Δ_a. The boundaries of the DOLS existence and stability are shown in Fig. 4. The stationary DOLS is stable in the central area, including the coordinate origin $\Delta_g = \Delta_a = 0$. The stability boundaries are given by curves 1 and 2. At the saddle-node bifurcation curves 2, a stable DOLS merges with an unstable one and disappears. We found also an additional bifurcation that is not shown in Fig. 4, since it is very close to the upper part of curves 2. At the Andronov-Hopf bifurcation curves labeled 1 there is a pair of pure imaginary eigenvalues λ, corresponding to even perturbations. In this case, destabilization of a stationary DOLS results in the arising of spatially inhomogeneous nonstationary regimes. Examples of such a regime, obtained by a numerical solution of Eq. (2.9), are given in Fig. 5. At the point of the Andronov-Hopf bifurcation, the period of DOLS oscillations is $2\pi/\mathrm{Im}\,\lambda$. It should be particularly emphasized that here we study an Andronov-Hopf bifurcation of an inhomogeneous (localized) field distribution, contrary to instabilities of homogeneous distributions (see, e.g., Refs. [6,14,33]). Periodically oscillating DOLS's

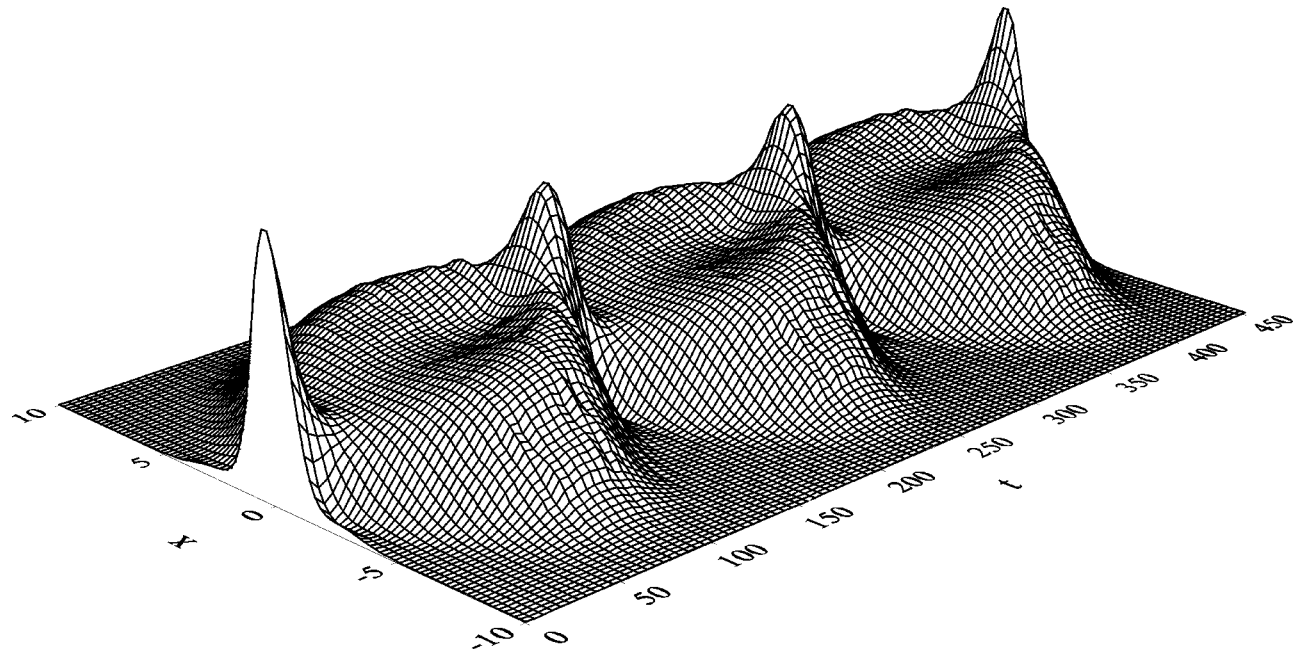

FIG. 5. Oscillatory localized structures $\Delta_g = 0.1$, and $\Delta_a = -0.48$. Other parameters are the same as in Fig. 2.

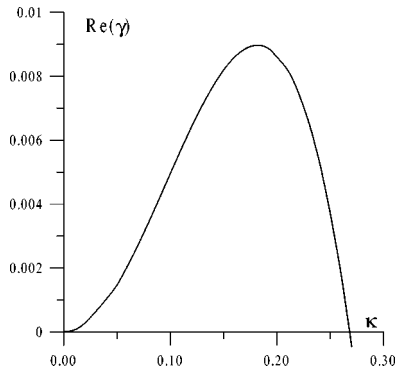

FIG. 6. Real part of the perturbation growth rate vs the spatial frequency κ: $g_0=2.06$, $a_0=2.0$, $b=10$, and $\Delta_{g,a}=0$.

exist between curves 3 and 4 in Fig. 4. Between curves 4 and 1 (lower curve) a more complex regime referred as a ''leading center'' arises. It is characterized by the periodical emerging of new (additional) DOLS's. Analogous regimes for zero frequency detunings were described in Ref. [34]. A similar bifurcation takes place near upper curve 1, but in a much more narrow domain. Note that Fig. 4 illustrates bifurcations of the fundamental DOLS, while its ''excited states'' with oscillating intensity transverse profile exist in a more narrow range of the laser parameters; see Ref. [26].

As pointed out above, we consider a transversely 1D laser with a single mode regime for the second transverse coordinate y. For transversely 2D lasers, there exist y-independent stripe patterns with the same field dependence on x as for the 1D laser. However, we have shown that these patterns are modulationally unstable. To find the small perturbation growth rate, one has to generalize expression (4.4) by inclusion of multipliers $\exp(\pm i\kappa y)$. The results of the growth rate calculation are presented in Fig. 6. The instability takes place in a finite range of perturbation spatial frequency κ. Different types of stable 2D DOLS's were described in Ref. [3].

V. EFFECT OF RELAXATION RATES

A. Transversely motionless dissipative structures

In this section we present numerical results concerning the stability of the motionless DOLS's as solutions of Eqs. (2.3a) with a zero value of the diffusion coefficient d and nonzero values of the population relaxation times $\tau_{g,a}>0$. Let us consider a slightly perturbed stationary DOLS [Eq. (4.1)] defined by Eq. (4.4), together with

$$\overline{g}(x,t)=g^{(0)}(x)+\delta g(x)e^{\lambda t}, \quad a(x,t)=a^{(0)}(x)+\delta a(x)e^{\lambda t}, \tag{5.1}$$

where $g^{(0)}(x)=\overline{g}(I(x))$ and $a^{(0)}(x)=\overline{a}(I(x))$ are given by Eq. (2.6). Here, as before, we choose the coordinate origin in such a way that the unperturbed DOLS envelope is an even function of the variable x [$A(x)=A(-x)$]. Due to this fact we can study the stability with respect to even (symmetric) and odd (antisymmetric) perturbations separately. Substituting Eqs. (4.4) and (5.1) into Eqs. (2.3b) and (2.3c), we obtain the linearized equation $\hat{L}\,\delta\mathbf{V}(x)=\lambda\,\delta\mathbf{V}(x)$ with $\delta\mathbf{V}(x)=(\mathrm{Re}\,\delta A,\mathrm{Im}\,\delta A,\delta g,\delta a)^T$.

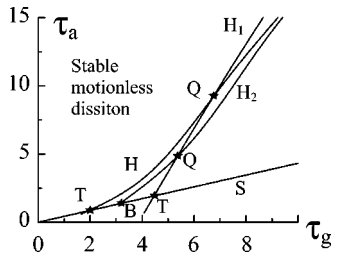

FIG. 7. Bifurcation diagram for the motionless localized structure: $g_0=2.06$, $a_0=2.0$, $b=10$, and $\Delta_{g,a}=0$. Bifurcation curves are obtained by means of numerical calculations of the discrete spectrum of the operator $\hat{L}$. The steady-state bifurcation line is marked S. Curves H, H_1, and H_2 correspond to Andronov-Hopf bifurcations. The motionless localized structure solution is stable above curves S, H, and H_1. Asterisks indicate the positions of codimension-two points.

As in the case of inertionless media, the operator $\hat{L}$ has two eigenvectors $\mathbf{\Psi}_1(x)=(-\mathrm{Im}\,A,\mathrm{Re}\,A,0,0)^T$ and $\mathbf{\Psi}_2(x)=\partial_x(\mathrm{Re}\,A,\mathrm{Im}\,A,g^{(0)},a^{(0)})^T$, which are associated with symmetries (2.10a) and (2.10b) respectively. However, the ''Galilean transformation'' symmetry (2.11) is now broken, and, as a result of this, the linear operator $\hat{L}$ has only two zero eigenvalues; $\lambda_1=\lambda_2=0$. The third eigenvalue λ_3, which was equal to zero in the inertionless limit $\tau_{g,a}=0$, is in the general case shifted from the origin in the complex plane. Therefore, even if the DOLS is stable for $\tau_{g,a}=0$, it may be unstable for arbitrary small nonzero relaxation times.

Bifurcation loci for the motionless DOLS as a solution of Eqs. (2.9) are shown in Fig. 7. They were plotted using the results of numerical calculation of the discrete spectrum of the operator $\hat{L}$. The straight line S indicates the steady-state bifurcation defined by the condition $\lambda_3=0$. Here the eigenvalue λ_3 corresponds to an odd eigenvector of the operator $\hat{L}$ which is different from $\mathbf{\Psi}_2$, but coincides with this eigenvector in the limit $\tau_{g,a}\to 0$. For sufficiently small $\tau_{g,a}$ the line S defines the stability boundary of the motionless DOLS. When crossing this line from the right, the motionless DOLS becomes unstable, giving rise to a localized structure slowly moving with some definite constant velocity v. The exact value of v depends on the distance from the instability boundary S. Since opposite directions of propagation are equivalent, there exist at least two DOLS's traveling with opposite velocities. If the population difference in the passive medium relaxes much faster than that in the active medium, the motionless DOLS is always unstable. Indeed, for $\tau_a=0$ and $\tau_g>0$ the passive medium is equally saturated by motionless and travelling DOLS's, while the active medium is less saturated by a travelling DOLS. This situation seems to be more favorable for the existence of a stable traveling DOLS than for a motionless one. With the increase of the relaxation time τ_a the absorption saturation decreases for a traveling DOLS, and for a given τ_g a certain threshold value of τ_a exists above which the motionless DOLS becomes stable. Thus the population relaxation process in an absorbing medium exerts a stabilizing effect on the motionless DOLS. When $\tau_{g,a}$ are large enough, different bifurcation scenario leading to the instability of the motionless DOLS is observed. In this case the stability boundary is associated with the Andronov-Hopf bifurcation. In Fig. 7 the

Andronov-Hopf bifurcation curves are marked H, H_1, and H_2. The curve H represents an Andronov-Hopf bifurcation with a pair of pure imaginary eigenvalues corresponding to even eigenvectors $[\mathbf{V}(x)=\mathbf{V}(-x)]$. This bifurcation leads to an oscillating DOLS similar to that shown in Fig. 5.

Curves H_1 and H_2 correspond to Andronov-Hopf bifurcations with a pair of pure imaginary eigenvalues associated with odd eigenvectors of the linear operator $\hat{L}$. The bifurcation curve H_2 terminates at a codimension-2 point of Bogdanov-Takens type [35,36] marked B in Fig. 7. Codimension-2 points associated with the interaction between two Andronov-Hopf bifurcations are also present in Fig. 7. These points are labeled Q. Under certain conditions the existence of this kind of degenerate bifurcation implies the appearance of quasiperiodic and irregular regimes [35]. Points T denote the intersections of the Andronov-Hopf bifurcation curves H and H_1 with the pitchfork bifurcation line S. These points correspond to codimension-2 bifurcations with a single zero and two purely imaginary eigenvalues.

B. Bifurcation to a slowly moving localized structure

In this section we derive an analytical stability condition for motionless DOLS's as solutions of Eqs. (2.3a) and (2.4), with nonzero values of relaxation times $\tau_{g,a}$. To this end, we introduce a perturbation technique for DOLS's with small transverse velocities and $d\neq 0$. We start with the laser equations in a moving frame of reference. Substituting, in Eqs. (2.3a) and (2.4),

$$\overline{E}(x,t)\rightarrow E(\xi)e^{iv\xi/2-iv\tau},\quad \overline{g}(x,t)\rightarrow g(\xi),\quad \overline{a}(x,t)\rightarrow a(\xi),$$

where $\xi=x-vt$, v is the velocity of moving frame accompanying the moving DOLS, ν is the nonlinear frequency shift for motionless DOLS, and $\alpha=\nu+(v^2/4)$, we obtain

$$-ivd(g,a)\frac{dE}{d\xi}+\frac{v^2}{4}d(g,a)E=i\alpha E+[i+d(g,a)]\frac{d^2E}{d\xi^2}+f(g,a)E, \tag{5.2a}$$

$$-\tau_g v\frac{dg}{d\xi}=\overline{g}_0-g-|E|^2g,\quad -\tau_a v\frac{da}{d\xi}=\overline{a}_0-a-\overline{b}|E|^2a, \tag{5.2b}$$

$$f(g,a)=-1+(1-i\Delta_g)g-(1-i\Delta_a)a,$$

$$d(g,a)=-2\left(\tau_{\perp g}g\frac{\Delta_g}{1+\Delta_g^2}-\tau_{\perp a}a\frac{\Delta_a}{1+\Delta_a^2}\right). \tag{5.2c}$$

We are looking for slowly moving DOLS's which can bifurcate from the motionless one. Let $\tau_g^{(0)}$ be the bifurcation value of the parameter τ_g corresponding to instability of the motionless DOLS. Then, perturbing the parameter τ_g near the bifurcation point, we obtain

$$\tau_g=\tau_g^{(0)}+v^2\tau_g^{(2)}.$$

Here the small parameter v is the velocity of the slowly moving DOLS to be found. The parameter $\tau_g^{(2)}$ measures the deviation from the bifurcation point.

Substituting Eqs. (5.2b) and (5.2c) into Eq. (5.2a), we obtain

$$i\alpha E+[i+d(|E|^2)]\partial_{\xi\xi}E+Ef(|E|^2)=-vU(E,\partial_\xi g,\partial_\xi a)+ivd(|E|^2)\partial_\xi E+\mathcal{O}(v^2\tau_{\perp g,\perp a}),$$

where $\partial_\xi\equiv d/d\xi$, $\partial_{\xi\xi}\equiv d^2/d\xi^2$, functions f and d are defined by Eq. (2.8), and

$$U(E,g,a)=E\left[\frac{(1-i\Delta_g)\tau_g g}{1+|E^2|}-\frac{(1-i\Delta_a)\tau_a a}{1+\overline{b}|E|^2}\right].$$

We are looking for slowly moving DOLS's in the forms

$$E(\xi)=E_0(\xi)+vE_1(\xi)+O(v^2),$$

$$g(\xi)=g^{(0)}(\xi)+vg^{(1)}(\xi)+O(v^2),$$

$$a(\xi)=a^{(0)}(\xi)+va^{(1)}(\xi)+O(v^2),$$

where $E_0(x)e^{-i\alpha t}$, $g^{(0)}(x)$, and $a^{(0)}(x)$ correspond to a motionless DOLS. Since the original equations are invariant under the transformation $(x,v)\rightarrow(-x,-v)$, for the fundamental DOLS we obtain $E_k(-\xi)=(-1)^kE_k(\xi)$, $g^{(k)}(-\xi)=(-1)^kg^{(k)}(\xi)$, $a^{(k)}(-\xi)=(-1)^ka^{(k)}(\xi)$, and $k=0$ and 1. Equating zeroth order terms in v, we obtain

$$g^{(0)}(\xi)=\frac{\overline{g}_0}{1+|E_0(\xi)|^2},\quad a^{(0)}(\xi)=\frac{\overline{a}_0}{1+\overline{b}|E_0(\xi)|^2}, \tag{5.3}$$

where the envelope of the motionless DOLS $E_0(x)$ obeys the equation

$$i\alpha E_0+[i+d(|E_0(\xi)|^2)]\partial_{\xi\xi}E_0+E_0f(|E_0(\xi)|^2)=0.$$

Equating the first order terms in v, we obtain

$$\hat{L}\mathbf{V}_1=\mathbf{U}_1, \tag{5.4}$$

where

$$\mathbf{V}_1=\begin{pmatrix}E_1\\ E_1^*\end{pmatrix},$$

$$\mathbf{U}_1=\begin{pmatrix}U(E_0,\partial_\xi g^{(0)},\partial_\xi a^{(0)})-id(|E_0|^2)\partial_\xi E_0\\ U^*(E_0,\partial_\xi g^{(0)},\partial_\xi a^{(0)})+id(|E_0|^2)\partial_\xi E_0^*\end{pmatrix}$$

and

$$\hat{L}=\begin{pmatrix} L_{11} & L_{12} \\ L_{12}^{*} & L_{11}^{*} \end{pmatrix}, \quad \begin{aligned} L_{11}&=-i\alpha-(i+d(I_0))\partial_{\xi\xi}-f(I_0)-I_0\partial_I f(I_0)-E_0^{*}\partial_{\xi\xi}E_0\partial_I d(I_0), \\ L_{12}&=-E_0^2\partial_I f(I_0)-E_0\partial_{\xi\xi}E_0\partial_I d(I_0), \end{aligned} \tag{5.5}$$

with $\partial_I f(I_0)=[df(I)/dI)_{I=I_0}$, and $I_0=|E_0|^2$.

Note that the linear operator $\hat{L}$ has zero eigenvalue associated with the eigenvector $\mathbf{\Psi}_1$ defined by

$$\mathbf{\Psi}_1=\begin{pmatrix} \psi_1 \\ \psi_1^{*} \end{pmatrix}, \quad \psi_1=\partial_\xi E_0, \quad \psi_1(\xi)=-\psi_1(-\xi).$$

These vectors obey the relations $\hat{L}\mathbf{\Psi}_1=0$. The adjoint operator $\hat{L}^{\dagger}$, which is obtained from Eq. (5.5) by transposition, has a zero eigenvalue associated with the eigenvectors $\mathbf{\Psi}_1^{\dagger}=(\psi_1^{\dagger},\psi_1^{\dagger *})^T$, and $\psi_1^{\dagger}(\xi)=-\psi_1^{\dagger}(-\xi)$. In order for Eq. (5.4) to be solvable, its right hand side must be orthogonal to the solution of the adjoint equation $\hat{L}^{\dagger}\mathbf{\Psi}_1^{\dagger}=0$:

$$\langle \mathbf{\Psi}_1^{\dagger}\mathbf{U}_1\rangle=0. \tag{5.6}$$

Equation (5.6) can be rewritten in the form

$$\begin{aligned} \tau_g^{(0)}\int_{-\infty}^{\infty}\frac{\mathrm{Re}[(1-i\Delta_g)E_0\psi_1^{\dagger}]\partial_\xi g^{(0)}}{1+|E_0|^2}d\xi \\ =\tau_a\int_{-\infty}^{\infty}\frac{\mathrm{Re}[(1-i\Delta_a)E_0\psi_1^{\dagger}]\partial_\xi a^{(0)}}{1+\overline{b}|E_0|^2}d\xi \\ +\int_{-\infty}^{\infty}d(|E_0|^2)\mathrm{Im}(\psi_1^{\dagger}\partial_\xi E_0)d\xi, \end{aligned} \tag{5.7}$$

with $g^{(0)}$ and $a^{(0)}$ defined by Eq. (5.3). Equation (5.7) defines the pitchfork bifurcation of a motionless DOLS into a slowly moving one, and corresponds to a straight line in the plane of parameters (τ_g,τ_a). According to Fig. 7, this line is the stability boundary of the motionless DOLS for moderate values of τ_g and τ_a.

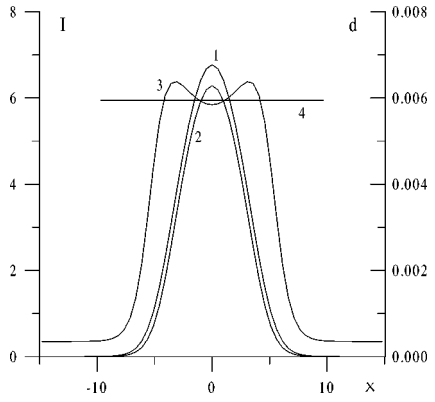

FIG. 8. Comparison of the ''exact'' (curves 1 and 3) and approximate (curves 2 and 4) stationary localized structures as solutions of Eq. (2.7). Transverse profiles of intensity I (curves 1 and 2) and diffusion coefficient d (curve 3 and line 4) for stable localized structures are given for $\tau_{\perp g,\perp a}=0.03$ and $\Delta_{g,a}=-0.1$. Other parameter values are the same as in Fig. 2.

C. Numerical simulations

Here we present the results of study of DOLS stability and bifurcations by numerical solution of Eqs. (2.3a). In Fig. 8 we show the transverse profile of the intensity dependent diffusion coefficient $d(I)$ (curve 3), and give its approximation by a constant value estimated in the vicinity of the DOLS intensity maximum (line 4). Curves 1 and 2 present DOLS transverse intensity profiles calculated for intensity dependent diffusion coefficient $d(I)$ defined by Eq. (2.8b), and for constant diffusion coefficient $d(I)=d=\mathrm{const}$, respectively. It follows from Fig. 8 that the approximation of constant diffusion coefficient does not change the DOLS shape essentially. Hence, when solving Eq. (2.7), one can assume that d is intensity independent.

Our numerical simulations based on Eqs. (2.3a) confirm the results of the bifurcation analysis given in Sec. V B. Additionally, they permit one to study dynamical regimes far from the bifurcation threshold, and, what is especially important, to find new types of DOLS's.

Stability domains of different types of DOLS's in the (τ_g,τ_a) plane are shown in Fig. 9. Steady-state motionless DOLS's are stable to the left of straight line 1 and curve 2. As discussed in Sec. V B, line 1 [see Eq. (5.7)] indicates a pitchfork bifurcation from a motionless DOLS into a slowly moving one. The latter type of DOLS is stable in the domain between straight line 1 and curve 3. The pitchfork bifurcation at line 1 is associated with an eigenvalue corresponding to an odd vector $\mathbf{\Psi}_3(x)=-\mathbf{\Psi}_3(-x)$. Therefore, unlike the motionless DOLS, the slowly moving one is transversely asymmetric. In other words, leading and trailing edges of a DOLS, which moves in a medium with relaxation, interact with unsaturated and saturated amplification and absorption, respectively. However, when the DOLS velocity is small,

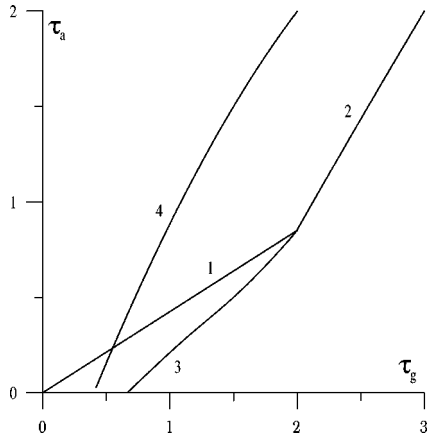

FIG. 9. Stability domains of different localized structures. Motionless localized structures are stable to the left from curves 1 and 3. Fast localized structures are stable to the right of curve 4. The slowly moving localized structure is stable between curves 1 and 3. Parameters are $d=0.01$ and $\Delta_g=\Delta_a=0$. Other parameters are the same as in Fig. 2.

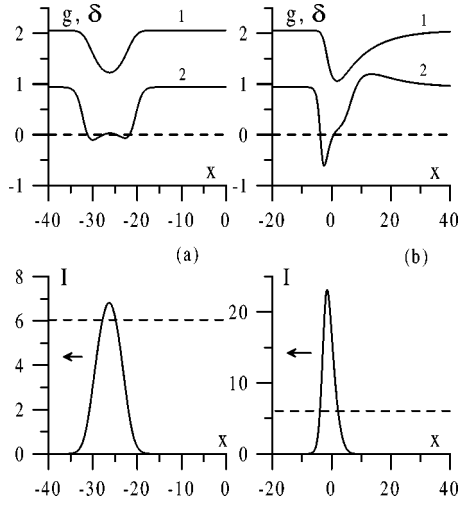

FIG. 10. Transverse profiles of radiation intensity I, population difference in active medium g (curve 1), and effective losses $\delta = 1 + a - g$ (curve 2) for a localized structure moving with velocity $v = -0.1036$ (a) and -9.367 (b). Dashed lines indicate intensity of the stationary spatially homogeneous states. Arrows indicate the direction of the localized structure motion. Parameters are $\tau_a = 0.3$ and $\tau_g = 1$. Other parameters are the same as in Fig. 9.

this asymmetry is practically indistinguishable. At the Andronov-Hopf bifurcation curve 2 transition from a motionless steady-state DOLS into a pulsating one occurs. This DOLS is similar to that shown in Fig. 5.

Numerical simulations revealed the existence of two different types of DOLS's. First, to the right of curve 4, stable DOLS's moving with large transverse velocity (''fast DOLS's'') can be formed. These structures are characterized by narrower intensity distributions and much greater peak intensities, as compared with slowly moving DOLSs. In Fig. 10 we present transverse profiles of the laser field intensity together with the saturated gain g and the difference between total losses and gain $1 + a - g$ for bistable ''slow'' and ''fast'' localized structures. It follows from this picture that at the leading edge of the fast DOLS the gain is practically unsaturated. The peak of the gain saturation is shifted to the trailing edge. Behind the core of the fast DOLS, there exists a ''refractory period'' zone [10], in which the gain slowly relaxes to its unsaturated value. Note that the peak intensity of the fast DOLS is much greater than the intensity of the homogeneous steady-state solution which corresponds to the upper branch of the bistability curve (see Fig. 1). This property establishes a certain similarity of the fast DOLS's with Q-switching regimes typical of lasers with a saturable absorber.

Second, DOLS's with a periodically varying transverse velocity and an oscillating transverse profile can be excited. Periodic evolution of the DOLS's characteristics is illustrated in Fig. 11. For the parameters of Fig. 11 the period of oscillations is $T = 50\tau_{\tilde{n}}$, where $\tau_{\tilde{n}}$ is the photon lifetime in the cavity.

Different types of DOLS's can coexist in certain parameter domains. A hysteretic behavior that takes place with the change of the population relaxation time in an amplifying medium, is illustrated by Fig. 12. Up to $\tau_g = 0.9$, a motionless DOLS is stable. With an increase of τ_g, this DOLS loses stability, and a slowly moving DOLS arises. The velocity of

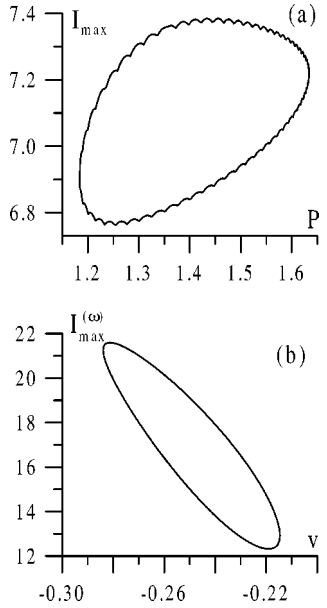

FIG. 11. Phase portrait of a localized structure with periodically oscillating velocity. $I_{\max}$ is the maximum radiation near-field intensity, P is the total power (a), $I^{(\omega)}_{\max}$ is the maximum far-field intensity, and v is the localized structure velocity (b). Parameters are: $\tau_a = 0.3$ and $\tau_g = 1.23$. Other parameters are the same as in Fig. 9.

a slow DOLS increases with τ_g up to a bifurcation into a DOLS with oscillating velocity at $\tau_g = 1.2$. As the relaxation time τ_g is further increased, a hysteretic jump to a branch corresponding to fast DOLS's occurs. Then, with a decrease of τ_g, a jump from the branch of the fast DOLS's to the branch of the motionless ones takes place at $\tau_g = 0.9$.

VI. CONCLUSION

We have performed a systematic study of the effect of frequency detunings on the properties of DOLS's—localized structures of coherent radiation in dissipative nonlinear optical schemes. In the limit of fast (inertionless) nonlinearity, the model considered describes both transversely 1D (slab) lasers with a saturable absorber and single mode fibers with gain and saturable losses. We have analyzed bifurcations of stationary DOLS's, and found a wide domain of detunings where periodically oscillating DOLS's and more complex spatially inhomogeneous nonstationary regimes arise. A hys-

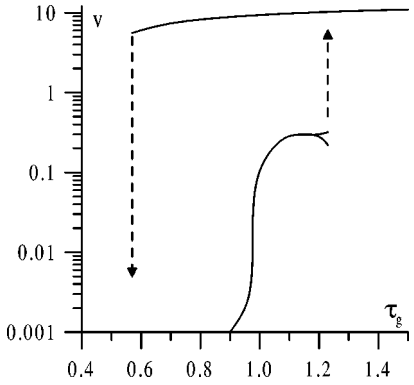

FIG. 12. Hysteretic change of the localized structure velocity for $\tau_a = 0.3$. Other parameters are the same as in Fig. 9.

teresis between stationary and nonstationary DOLS's was demonstrated.

Important new features of the DOLS's arise when the relaxation processes in intracavitary active and passive media are taken into account. We present a derivation of the field envelope equation, which includes intensity-dependent effective diffusion coefficient. Linear stability analysis of the simplest transversely motionless DOLS's revealed the conditions of bifurcations of these DOLS's into slowly moving or pulsating ones. Secondary bifurcations of the pulsating DOLS's lead to more complex patterns, with a nonconservation of the number of localized structures. Numerical solution of the envelope equation shows the existence of two new types of DOLS's: (i) fast DOLS's, i.e., DOLS's moving with large transverse velocity which are similar to *Q*-switching regimes in a laser with a saturable absorber; and (ii) DOLS's characterized by a transverse velocity and profile oscillating in time. With a change of the laser parameters, hysteretic jumps between different types of DOLS's occur.

The results presented demonstrate the existence of a large variety of localized structures in dissipative optical systems under bistability conditions. Although only 1D structures were studied here, similar features are expected for two- and three-dimensional DOLS's.

ACKNOWLEDGMENT

This work was supported by the ISTC under Project No. 666.

[1] G. Nicolis and I. Prigogine, *Self Organization in Nonequilibrium Systems* (Wiley, New York, 1977).
[2] H. Haken, *Synergetics—An introduction* (Springer-Verlag, Berlin, 1977).
[3] N. N. Rosanov, *Optical Bistability and Hysteresis in Distributed Nonlinear Systems* (Nauka, Moscow, 1997).
[4] N. N. Akhmediev and N. Ankiewicz, *Solitons: Nonlinear Pulses and Beams* (Chapman & Hall, London, 1997).
[5] N. N. Rosanov and G. V. Khodova, Opt. Spektrosk **65**, 1375 (1988) [Opt. Spectrosc. **65**, 1399 (1988)].
[6] N. N. Rosanov, A. V. Fedorov, and G. V. Khodova, Phys. Status Solidi B **150**, 545 (1988).
[7] A. N. Rakhmanov, Opt. Spektrosk. **74**, 1184 (1993).
[8] A. N. Rakhmanov and V. I. Shmalhausen, Proc. SPIE **2108**, 428 (1993).
[9] N. N. Rosanov, in *Progress in Optics*, edited by E. Wolf (Elsevier, Amsterdam, 1996), Vol. 35, p. 1.
[10] V. A. Vasil'ev, Yu. M. Romanovskii, and V. G. Yakhno *Autowave Processes* (Nauka, Moscow, 1979).
[11] B. S. Kerner and V. V. Osipov, *Autosolitons* (Nauka, Moscow, 1991).
[12] B. A. Malomed, Physica D **29**, 155 (1987).
[13] M. C. Cross and P. C. Hohenberg, Rev. Mod. Phys. **65**, 851 (1993).
[14] M. Tlidi, Paul Mandel, and R. Lefever, Phys. Rev. Lett. **73**, 640 (1994).
[15] L. Spinelli, G. Tissoni, M. Brambilla, F. Prati, and L. A. Lugiato, Phys. Rev. A **58**, 2542 (1998).
[16] S. V. Fedorov and N. N. Rosanov, Opt. Spektrosk. **72**, 1394 (1992).
[17] M. Saffman, D. Montgomery, and D. Z. Anderson, Opt. Lett. **19**, 518 (1994).
[18] G. Slekys, K. Staliunas, and C. O. Weiss, Opt. Commun. **149**, 113 (1998).
[19] V. B. Taranenko, K. Staliunas, and C. O. Weiss, Phys. Rev. A **56**, 1582 (1997).
[20] N. N. Rosanov, A. V. Fedorov, S. V. Fedorov, and G. V. Khodova, Zh. Éksp. Teor. Fiz. **107**, 376 (1995) [JETP **80**, 199 (1995)].
[21] N. N. Rosanov, A. V. Fedorov, S. V. Fedorov, and G. V. Khodova, Physica D **96**, 272 (1996).
[22] N. A. Kaliteevskii, N. N. Rosanov, and S. V. Fedorov, Opt. Spektrosk. **85**, 533 (1998) [Opt. Spectrosc. **85**, 485 (1998)].
[23] J. M. Soto-Crespo, N. N. Akhmediev and V. V. Afanasjev, J. Opt. Soc. Am. B **13**, 1439 (1996); N. N. Akhmediev, A. Ankiewicz, and J. M. Soto-Crespo, Phys. Rev. Lett. **79**, 4047 (1997).
[24] S. V. Fedorov and N. N. Rosanov, Kvant. Electron (Moscow) **27**, 175 (1995) [Quantum Electron. **29**, 454 (1999).
[25] E. A. Vanin *et al.*, Phys. Rev. A **49**, 2806 (1994).
[26] A. G. Vladimirov, N. N. Rosanov, S. V. Fedorov, and G. V. Khodova, Kvant. Elektron (Moscow) **24**, 978 (1997) [Quantum Electron. **27**, 949 (1997)]; **25**, 58 (1998) [**28**, 55 (1998)].
[27] A. F. Suchkov, Zh. Éksp. Teor. Fiz. **49**, 1495 (1965) [Sov. Phys. JETP **22**, 1026 (1966)].
[28] K. Staliunas, Phys. Rev. A **48**, 1573 (1993).
[29] P. Mandel, *Theoretical Problems in Cavity Nonlinear Optics* (Cambridge University Press, Cambridge, England, 1997).
[30] A. G. Vladimirov, S. V. Fedorov, N. A. Kaliteevskii, G. V. Khodova, and N. N. Rosanov, J. Opt. B: Quantum Semliclass. Opt. **1**, 101 (1999).
[31] N. N. Rosanov, Proc. SPIE **1840**, 130 (1991).
[32] N. N. Rosanov and G. V. Khodova, Opt. Spektrosk. **72**, 1403 (1992) [Opt. Spectrosc. **72**, 1394 (1992)].
[33] M. Tlidi and Paul Mandel, Phys. Rev. E **56**, 6524 (1997); Phys. Rev. A **59**, R2575 (1999).
[34] N. N. Rosanov, S. V. Fedorov, G. V. Khodova, and A. A. Zinchik, Opt. Spektrosk. **83**, 396 (1992) [Opt. Spectrosc. **83**, 370 (1997)].
[35] J. Guckenheimer and P. Holmes, *Nonlinear Oscillations, Dynamical Systems and Bifurcations of Vector Fields* (Springer, Heidelberg, 1983).
[36] V. I. Arnold, *Geometrical Methods in the Theory of Ordinary Differential Equations* (Springer, Heidelberg, 1983).